

Balancing Climate Mitigation and Adaptation: A Dynamic Economic Assessment of Blue Carbon in the Venice Lagoon

SUPPLEMENTARY INFORMATION

Sebastian Raimondo^{1,*}, Federico Cornacchia^{1,2}, Perla Irasema Rivadeneyra García^{1,3}, and Carlo Giupponi^{1,3,*}

¹Fondazione Eni Enrico Mattei, ADAPT@VE, Venice, 30124, Italy

²Ca' Foscari University of Venice, Department of Environmental Sciences, Informatics and Statistics , Venice, Italy

³Ca' Foscari University of Venice, Department of Economics, Venice, Italy

*sebastian.raimondo@feem.it

*carlo.giupponi@feem.it

MoSE operational dynamics and lagoon water level estimation

To evaluate the long-term impacts of alternative sea-level management strategies in the Venice Lagoon, we implemented a rule-based simulation of the MoSE barrier system. The control logic was designed to emulate decision-making under forecast uncertainty through a pseudo-prediction approach. At each time step t —corresponding to six hours, in line with the characteristic tidal cycle in the lagoon—the decision to open or close the barriers is based on a pseudo-predicted offshore sea level at time $t + 1$. This pseudo-forecast is generated by shifting the observed time series forward by one time step and perturbing it with Gaussian noise to reproduce the uncertainty typical of the real-time forecast¹. This framework allows for four decision points per simulated day, aligning with the natural tidal oscillations and the temporal resolution of operational assessments. The simulation was applied to long-term sea-level projections under RCP2.6 and RCP8.5 scenarios.

At each decision point, if the MoSE is open and the pseudo-predicted sea level at the offshore ISMAR-CNR platform exceeds a specified threshold (either 1.1 m or 1.3 m a.s.l.), the barriers are closed at the subsequent time step. Once the system is closed, the lagoon is hydraulically decoupled from the Adriatic, and its internal sea level is no longer driven by external tidal dynamics. Instead, it is estimated via a linear empirical model relating sea levels at Piattaforma CNR and Punta della Salute. This model, calibrated on historical observations, takes the form:

$$\text{Level}_{\text{Lagoon}} = \text{Level}_{\text{CNR}} + \alpha + \beta \cdot \text{Level}_{\text{CNR}},$$

with coefficients $\alpha = 0.981$ and $\beta = -1.176$, and an associated coefficient of determination of $R^2 = 0.70$. Importantly, this statistical relationship captures not only the mean tidal gradient between the sea and the lagoon but also partially incorporates the effects of meteorological forcing (e.g., wind setup, atmospheric pressure) and operational heuristics that can cause significant deviations from a purely threshold-based response.

The decision rule is symmetric: if the MoSE is closed and the pseudo-predicted offshore level falls below the defined threshold, the barriers reopen at the next time step, and the lagoon level resumes tracking the open-sea level at Piattaforma CNR.

Salt marsh elevation discretization

To represent the elevation-dependent behaviour of salt marshes within our system dynamics model, we discretized the continuous bathymetry into classes using unsupervised clustering. Elevation data were extracted from a high-resolution digital elevation model (10 m spatial resolution) and masked using a shapefile of natural salt marshes to isolate relevant areas.

The extracted elevation values were then classified using a k-means algorithm ($k = 7$). This data-driven approach yielded a set of distinct elevation bands, each defined by a centroid value. For each class, the total area was computed by multiplying the number of cells assigned to the class by the area of the cell. The resulting distribution preserves the morphological heterogeneity of the salt marsh platform and serves as an effective and compact representation of vertical diversity for subsequent dynamic modelling.

A spatial representation of the clustered elevation classes is shown in Fig. 1, illustrating the fragmented and spatially heterogeneous character of the lagoon's salt marsh landscape.

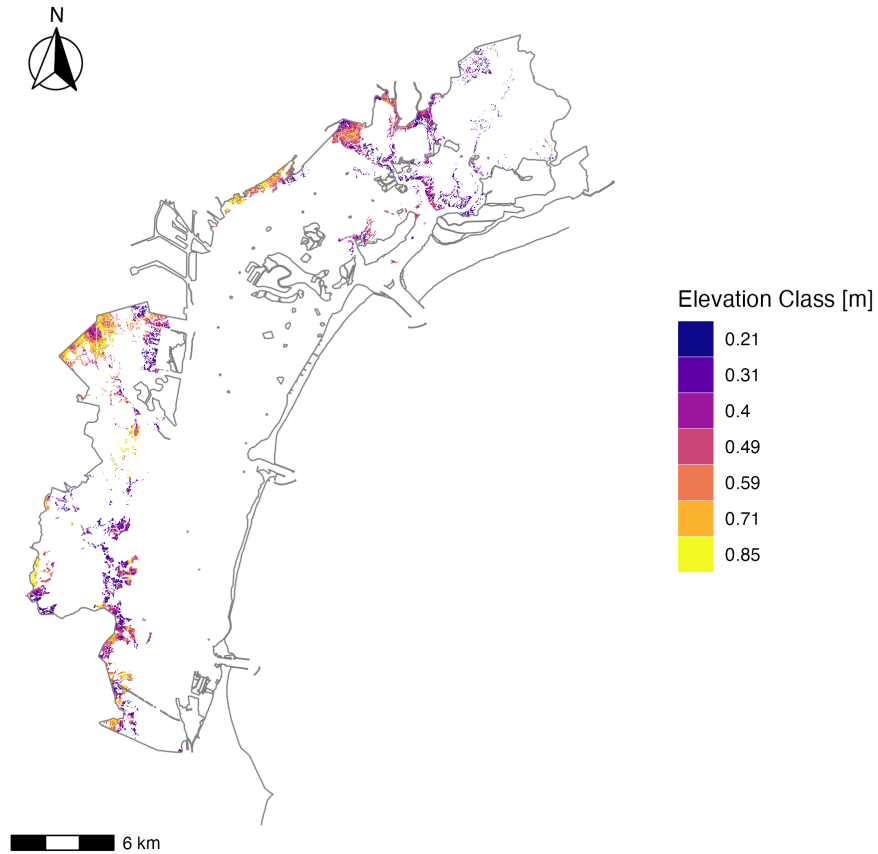


Figure 1. Spatial distribution of clustered salt marsh elevation classes across the Venice Lagoon. Elevation classes are derived via *k*-means clustering and displayed in color scale from lower (blue) to higher (yellow) elevations.

Sedimentation

Figure 2 presents the daily sedimentation rate per square meter of salt marsh (upper panels) and the annual carbon accumulation rate per km^2 of lagoon surface (lower panels) across different initial elevation classes and management scenarios. As expected, sedimentation rates decrease with increasing initial elevation, as higher marsh surfaces experience shorter inundation periods, reducing sediment deposition. This pattern is consistent across all management scenarios, although variations emerge depending on MoSE activation thresholds. In the 1.1 m management scenario, sedimentation rates are relatively stable across climate scenarios (RCP 2.6 and RCP 8.5), with lower elevations exhibiting the highest accumulation due to prolonged submersion. Increasing the MoSE activation threshold to 1.3 m enhances sedimentation at lower elevations, while higher elevations maintain lower rates, following the expected negative feedback between elevation and sediment deposition. In contrast, the No MoSE scenario results in overall higher sedimentation rates across all elevation classes, reflecting the uninterrupted exchange with the open sea and the increased frequency of sediment deposition events. The lower panels of Figure 2 illustrate the corresponding carbon accumulation rates, which closely follow sedimentation patterns. The estimates derived from our model align well with recent field-based measurements by Puppin et al.², who report an accumulation rate of approximately $85 \pm 25 \text{ ton OC km}^{-2} \text{ yr}^{-1}$. Under current conditions—assuming a 1.1 m closure threshold and RCP 2.6—our model estimates an average accumulation rate of $67.6 \text{ ton OC km}^{-2} \text{ yr}^{-1}$, which falls within the observed uncertainty range. Notably, in the No MoSE scenario, accumulation rates remain higher across all elevation classes, emphasizing the role of natural hydrodynamics in sustaining carbon sequestration. However, these estimates must be interpreted with caution, as the No MoSE scenario does not fully capture potential shifts in sediment dynamics under higher water levels. Tidal biomorphodynamics are shaped by complex feedbacks between vegetation, sedimentation, and hydrodynamics, which can lead to nonlinear responses and alternative stable states³. Under accelerated relative sea level rise (RSLR), prolonged inundation and increased wave energy may reduce

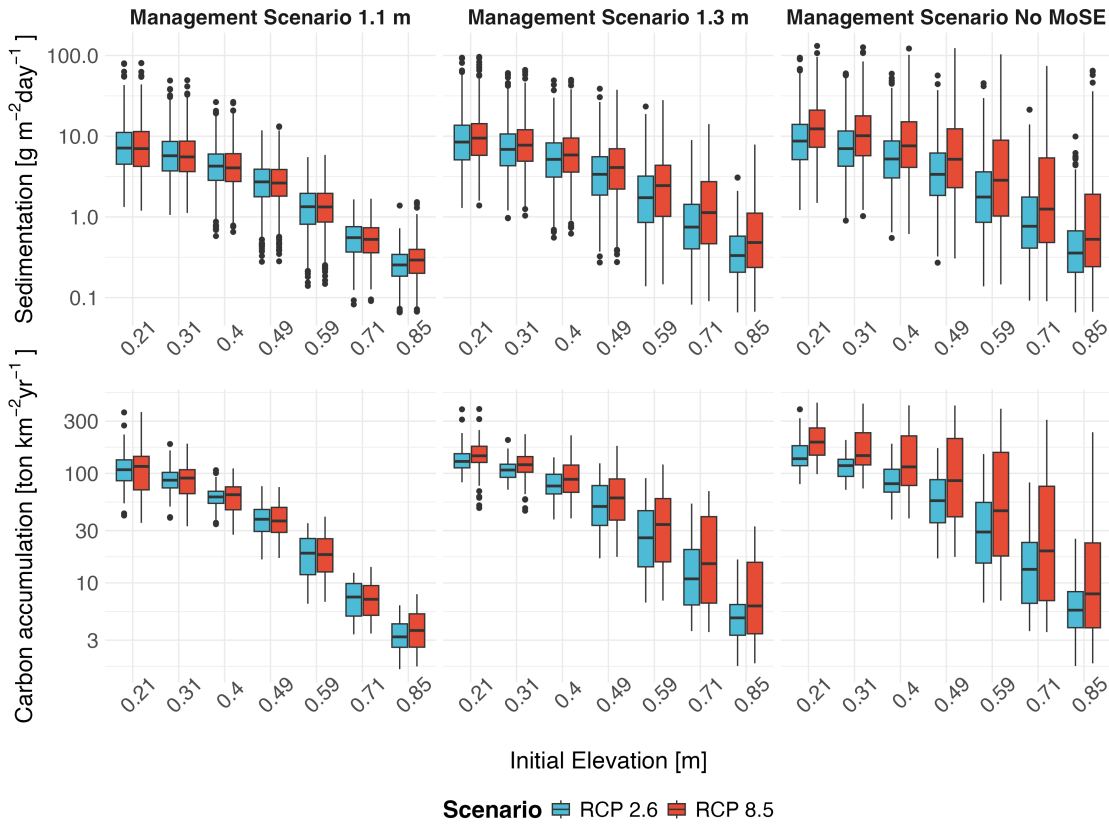


Figure 2. Sedimentation and carbon accumulation distribution divided by initial elevation class, over the entire time horizon 2025-2100. The upper panel shows the daily sedimentation rate estimated by the model for different initial elevation classes. As elevation increases, the mean inundation depth (MID) generally decreases, leading to a reduction in sedimentation rates.

Notably, the modeled values align with the calibration data from Tognin et al. (2021)⁴. The lower panel presents the corresponding annual carbon accumulation rate for the same elevation classes. These estimates are consistent with recent field-based measurements reported in Puppin et al. (2024)².

sediment trapping efficiency, weakening marsh resilience and enhancing lateral erosion. While our model captures the dominant sedimentation processes, it does not explicitly account for potential shifts in vegetation dynamics or biostabilization breakdown, which could further influence long-term carbon sequestration capacity.

For completeness, figure 3 shows the time series of the economic value of carbon accumulation (flow), calculated using the two per-ton price estimates provided in the main text.

Salt marsh areal erosion estimation

To represent salt marsh lateral erosion within a system dynamics model operating at lagoon scale, we employed a simplified but observation-driven approach. Although erosion processes vary spatially due to local morphology and hydrodynamics, our aim was to reproduce the long-term average dynamics of salt marsh loss, consistent with the aggregate scale of the model.

We relied on historical records of total salt marsh area in the Venice Lagoon, spanning from 1810 to 2014⁵⁻⁷. To capture stable, long-term trends, we identified two distinct temporal phases—1810–1901 and 1970–2014—during which erosion proceeded at a nearly constant rate. The intervening period (1901–1970) was excluded due to the abrupt and anomalous loss of marshes following major anthropogenic alterations, including the excavation of navigation channels, port expansion, and modifications to lagoon inlets. These interventions caused a sharp drop in salt marsh area, breaking the otherwise linear pattern of decline.

Linear regressions were fitted separately to the two retained intervals. Despite being over a century apart, both regressions yielded almost identical slopes (-1.922 and -1.945 km^2 per year), suggesting a remarkably persistent erosion trend. The second regression (1970–2014), based on more recent and accurate data, was selected to project future areal loss under a business-as-usual scenario. Extrapolating this trend yields a vanishing year of $x_0 \approx 2225$, when the total marsh area would

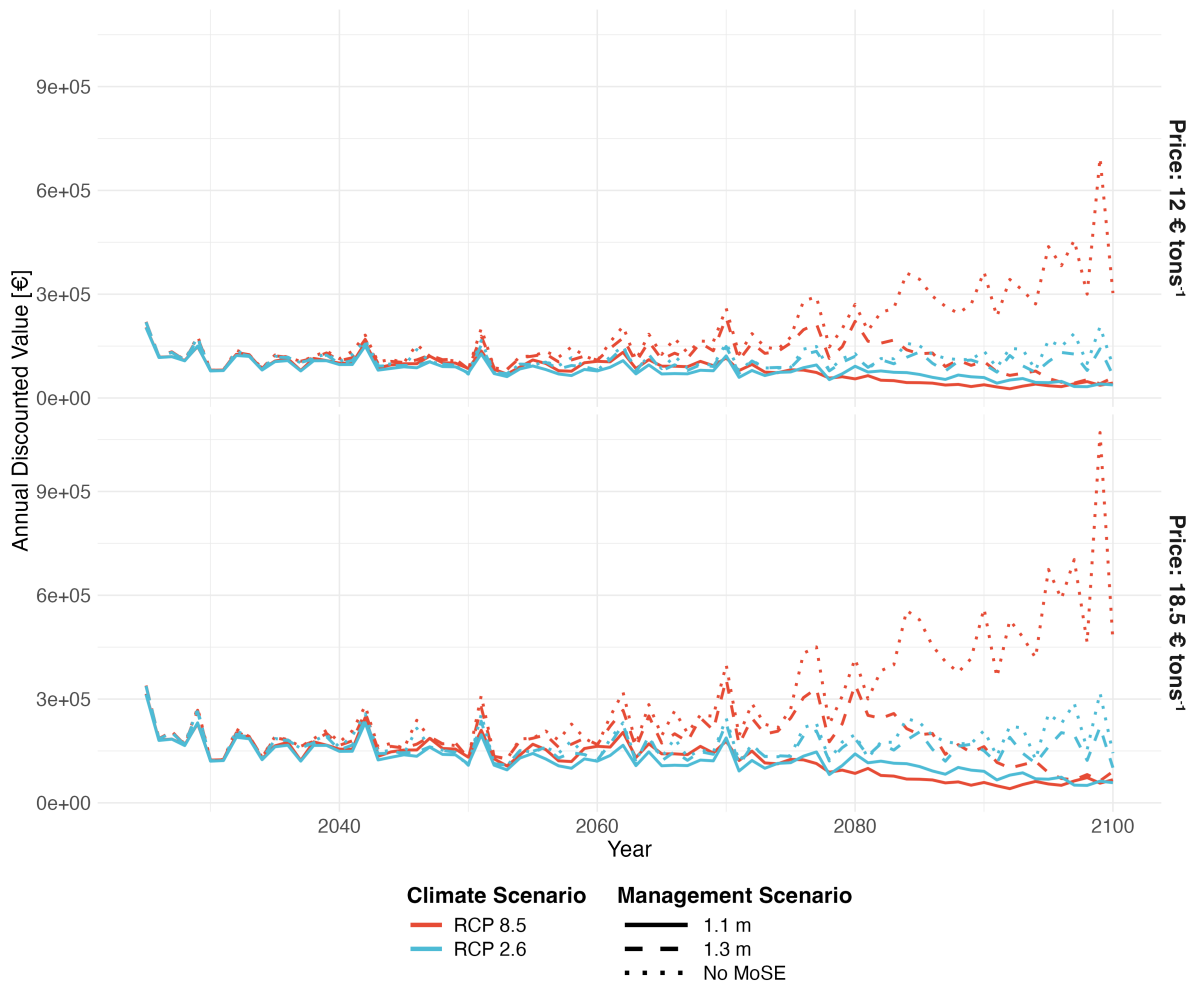


Figure 3. Annual economic value of carbon accumulation in the Venice Lagoon's salt marshes. The figure shows the evolution of carbon value until 2100 under different climate scenarios (RCP 2.6 and RCP 8.5) and MoSE management scenarios (1.1 m, 1.3 m, and No MoSE). The analysis considers two carbon prices (€12/ton and €18.5/ton).

reach zero. To remain consistent with the lumped structure of the model, we assumed that all elevation bands behave as a single cohesive body and erode uniformly over time. Accordingly, each class was assigned a linear loss rate that brings its area to zero in the year x_0 , starting from its observed value in 2014. This ensures coherence between elevation-specific erosion rates and the total observed trajectory of marsh decline.

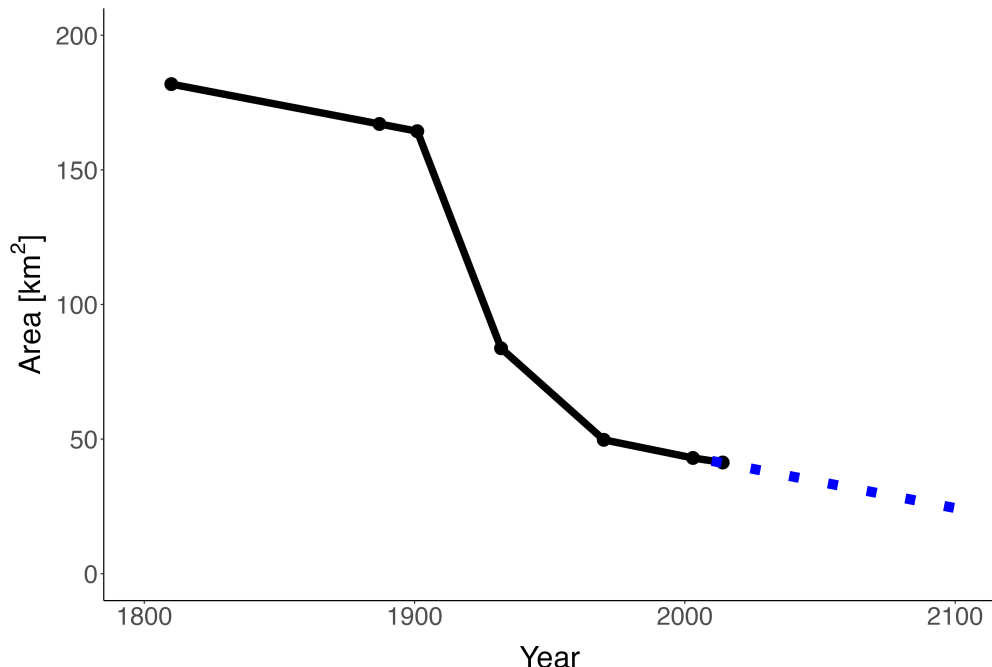


Figure 4. Historical and projected erosion trend for natural salt marshes in the Venice Lagoon. Black points represent observed total area from 1810 to 2014. The dashed blue line indicates the extrapolated trend based on the 1970–2014 regression.

References

1. Giupponi, C. *et al.* Boon and burden: economic performance and future perspectives of the venice flood protection system. *Reg. Environ. Chang.* **24**, 44 (2024).
2. Puppin, A. *et al.* Blue carbon assessment in the salt marshes of the venice lagoon: Dimensions, variability and influence of storm-surge regulation. *Earth's Futur.* **12**, e2024EF004715 (2024).
3. Marani, M., D'Alpaos, A., Lanzoni, S., Carniello, L. & Rinaldo, A. The importance of being coupled: Stable states and catastrophic shifts in tidal biomorphodynamics. *J. Geophys. Res. Earth Surf.* **115** (2010).
4. Tognin, D., D'Alpaos, A., Marani, M. & Carniello, L. Marsh resilience to sea-level rise reduced by storm-surge barriers in the venice lagoon. *Nat. Geosci.* **14**, 906–911 (2021).
5. Tommasini, L., Carniello, L., Ghinassi, M., Roner, M. & D'Alpaos, A. Changes in the wind-wave field and related salt-marsh lateral erosion: inferences from the evolution of the venice lagoon in the last four centuries. *Earth Surf. Process. Landforms* **44**, 1633–1646 (2019).
6. Finotello, A. *et al.* Hydrodynamic feedbacks of salt-marsh loss in the shallow microtidal back-barrier lagoon of venice (italy). *Water Resour. Res.* **59**, e2022WR032881 (2023).
7. D'Alpaos, L. *et al.* L'evoluzione storica della laguna di venezia attraverso la lettura di alcune mappe storiche e delle sue carte idrografiche. *Comune di Venezia* (2010).